Article

Cell Reports

Calorie-Restriction-Induced Insulin Sensitivity Is Mediated by Adipose mTORC2 and Not Required for Lifespan Extension

Graphical Abstract

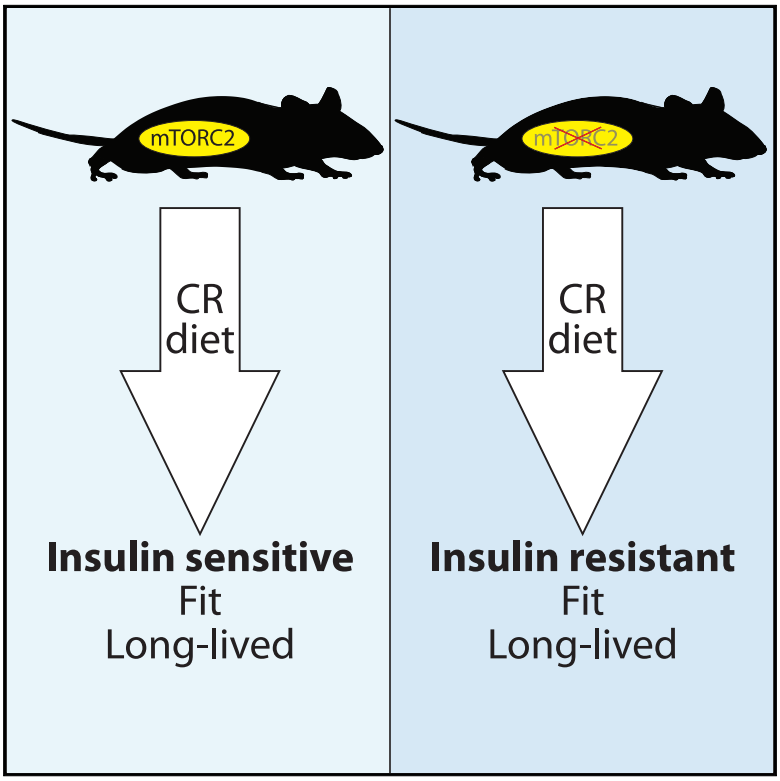

Authors

Deyang Yu, Jay L. Tomasiewicz, Shany E. Yang, ..., Jacqueline A. Brinkman, Faizan A. Syed, Dudley W. Lamming

Correspondence

dlamming@medicine.wisc.edu

In Brief

Calorie restriction (CR) diets improve insulin sensitivity and extend lifespan. Yu et al. find that although mice lacking mTORC2 in adipose remain insulin resistant on a CR diet, their fitness and longevity increases similarly to wild-type mice.

Highlights

- Calorie restriction (CR) extends lifespan and improves insulin sensitivity
- Mice lacking adipose mTORC2 are insulin resistant, even on a CR diet
- CR promotes fitness and longevity in mice lacking adipose mTORC2
- Improved organismal insulin sensitivity does not mediate the beneficial effects of CR

Yu et al., 2019, Cell Reports *29*, 236–248
October 1, 2019
https://doi.org/10.1016/j.celrep.2019.08.084

OPEN ACCESS
CellPress

Cell Reports
Article

Calorie-Restriction-Induced Insulin Sensitivity Is Mediated by Adipose mTORC2 and Not Required for Lifespan Extension

Deyang Yu,[1,2,3] Jay L. Tomasiewicz,[1] Shany E. Yang,[1,2] Blake R. Miller,[1,2] Matthew H. Wakai,[1,2] Dawn S. Sherman,[1,2] Nicole E. Cummings,[1,2,4] Emma L. Baar,[1,2] Jacqueline A. Brinkman,[1,2] Faizan A. Syed,[1,2] and Dudley W. Lamming[1,2,3,4,5,6,*]

[1]William S. Middleton Memorial Veterans Hospital, Madison, WI, USA
[2]Department of Medicine, University of Wisconsin-Madison, Madison, WI, USA
[3]Molecular and Environmental Toxicology Program, University of Wisconsin-Madison, Madison, WI, USA
[4]Endocrinology and Reproductive Physiology Graduate Training Program, University of Wisconsin-Madison, Madison, WI, USA
[5]University of Wisconsin Carbone Cancer Center, Madison, WI, USA
[6]Lead Contact
*Correspondence: dlamming@medicine.wisc.edu
https://doi.org/10.1016/j.celrep.2019.08.084

SUMMARY

Calorie restriction (CR) extends the healthspan and lifespan of diverse species. In mammals, a broadly conserved metabolic effect of CR is improved insulin sensitivity, which may mediate the beneficial effects of a CR diet. This model has been challenged by the identification of interventions that extend lifespan and healthspan yet promote insulin resistance. These include rapamycin, which extends mouse lifespan yet induces insulin resistance by disrupting mTORC2 (mechanistic target of rapamycin complex 2). Here, we induce insulin resistance by genetically disrupting adipose mTORC2 via tissue-specific deletion of the mTORC2 component *Rictor* (AQ-RKO). Loss of adipose mTORC2 blunts the metabolic adaptation to CR and prevents whole-body sensitization to insulin. Despite this, AQ-RKO mice subject to CR experience the same increase in fitness and lifespan on a CR diet as wild-type mice. We conclude that the CR-induced improvement in insulin sensitivity is dispensable for the effects of CR on fitness and longevity.

INTRODUCTION

Calorie restriction (CR), a dietary regimen in which calories are reduced without causing malnutrition, extends the lifespan of many diverse species and is the gold standard for interventions that promote the health and longevity of mammals (Lamming and Anderson, 2014; Madeo et al., 2019). Importantly, CR extends not only longevity but also healthspan, decreasing the incidence of age-related diseases, including cardiovascular disease, neurodegenerative disorders, cancer, and diabetes, and in addition reduces frailty (Kane et al., 2016; Balasubramanian et al., 2017). There has therefore been great interest in identifying the physiological and molecular mechanisms by which CR promotes health and longevity (Fontana and Partridge, 2015; López-Lluch and Navas, 2016; Speakman et al., 2016).

In mammals fed a CR diet, one of the most striking and broadly conserved effects is improved sensitivity to insulin (Lamming and Anderson, 2014; Most et al., 2017). Many dietary and pharmaceutical interventions that extend mammalian lifespan and healthspan likewise promote insulin sensitivity, while conversely, there is a well-known association of insulin resistance with diabetes and poor health. Given the central role of the insulin signaling pathway in the lifespan of worms, flies, and mammals (Lamming, 2014; Kenyon, 2001), improved insulin sensitivity has been proposed as an essential mechanism by which a CR diet extends mammalian lifespan (Lamming and Anderson, 2014). While the effects of CR are systemic, some of its most prominent effects are on adipose tissue; CR reduces adiposity in mammals, mobilizing fat stores in white adipose tissue (WAT) while also activating WAT lipogenesis, which is associated with improved systemic insulin sensitivity and metabolic health (Herman et al., 2012; Chen et al., 2008; Bruss et al., 2010).

Despite the strong correlative evidence that CR promotes health and longevity through improved insulin sensitivity, there is clear evidence that insulin sensitivity may not necessarily be essential for healthy aging. Several genetically modified mouse models in which insulin resistance has been induced in one or more tissues have extended lifespan (Blüher et al., 2003; Holzenberger et al., 2003; Selman et al., 2008), while mice treated with rapamycin, an inhibitor of the mTOR (mechanistic target of rapamycin) protein kinase that extends lifespan, develop insulin resistance in multiple tissues (Lamming et al., 2012). Correctly interpreting these results is difficult; for example, the FIRKO (fat insulin receptor knockout) mice retain insulin sensitivity at the organismal level, and the FIRKO mouse study was conducted utilizing Cre recombinase under the control of an *AP2* promoter, which is now known not to be specific for adipose tissue (Lee et al., 2013; Blüher et al., 2003).

Over the last decade, a critical role for mTOR complex 2 (mTORC2) in the control of organismal metabolism has become apparent. In contrast to the well-known mTOR complex 1 (mTORC1), which functions as a key integrator of many different environmental and hormonal cues, mTORC2 functions primarily

as an effector of phosphatidylinositol 3-kinase (PI3K) signaling, contributing to the downstream activation of many kinases, including AKT, by insulin (Sarbassov et al., 2005; Guertin et al., 2006). Deletion of *Rictor*, which encodes an essential protein component of mTORC2, results in insulin resistance in tissues, including liver, adipose tissue, and skeletal muscle (Cybulski et al., 2009; Kumar et al., 2008, 2010; Yuan et al., 2012; Hagiwara et al., 2012; Kleinert et al., 2017; Lamming et al., 2012, 2014a). The organismal consequences of inactivating adipose mTORC2 have been unclear, as distinct phenotypes have been observed in mice where *Rictor* was deleted using *AP2-Cre* and a more recent study utilizing the adipose-specific *Adiponectin-Cre* (Tang et al., 2016; Cybulski et al., 2009; Kumar et al., 2010). Published studies of the effects of adipose mTORC2 have also been limited to relatively young mice under 1 year of age.

While an important role for CR-induced insulin sensitivity in the health and survival benefits of CR has long been assumed, the contribution of improved insulin sensitivity to the benefits of CR has not been directly examined. Here, we have tested the role of CR-induced insulin sensitivity on the metabolic health, frailty, and longevity of mice by placing mice lacking adipose mTORC2 signaling (AQ-RKO: *Adiponectin-Cre; Rictor*$^{loxP/loxP}$) and their wild-type littermates on either *ad libitum* or CR diets. Critically, the insulin sensitivity of AQ-RKO mice does not improve on a CR diet, enabling us to discern the role of CR-induced insulin sensitivity in CR-induced phenotypes. Although the WAT of AQ-RKO mice has a blunted metabolic response to CR and female AQ-RKO mice fed an *ad libitum* diet have a slightly reduced lifespan, we find that AQ-RKO mice of both sexes fed a CR diet have increased fitness and extended lifespan. We conclude that the CR-induced increase in insulin sensitivity is dispensable for the effects of CR on fitness and longevity.

RESULTS

Deletion of Adipose *Rictor* Impairs Insulin Sensitivity

We generated adipose-specific *Rictor* knockout mice by crossing *Rictor* floxed mice with mice expressing Cre recombinase under the control of the adiponectin promoter (AQ-RKO; *Adipoq-Cre*; *Rictor*$^{loxP/loxP}$). As expected, we found that RICTOR protein expression was substantially reduced in the adipose tissues of AQ-RKO mice, including the inguinal WAT (iWAT) and epididymal WAT (eWAT), but was not altered in other organs, including liver and skeletal muscle (Figure 1A). Consistent with this, phosphorylation of the mTORC2 substrate AKT S473 was likewise significantly reduced in iWAT and eWAT, but not in other tissues (Figure 1A).

Adipose mTORC2 has been proposed to negatively regulate whole-body growth, as young *Ap2-Cre*; *Rictor*$^{loxP/loxP}$ mice have increased body weight and lean tissue mass with elevated IGF-1 (Cybulski et al., 2009). However, these phenotypes were not observed in mice in which *Rictor* was deleted using *Adiponectin-Cre* (Tang et al., 2016). In agreement with these latter results, we found that young AQ-RKO mice have approximately normal body weight (Figure 1B), with the mass of most AQ-RKO organs equivalent to that of their littermate controls (Figures 1C and 1D). However, the liver weight of female AQ-RKO mice was significantly greater than that of their littermate controls (Figure 1D); correlated with this, we found that plasma levels of IGF-1 were elevated in female AQ-RKO mice, but not in males (Figure 1E).

We also examined the effect of adipose mTORC2 loss on glucose homeostasis. We found that AQ-RKO mice of both sexes were glucose tolerant (Figure 1F), but, as we anticipated given the established role of adipose tissue in insulin-stimulated glucose clearance (Rosen and Spiegelman, 2006), we observed that AQ-RKO mice were insulin resistant, with a more pronounced effect in male mice (Figure 1G).

Adipose mTORC2 Is Required for CR to Improve Insulin Sensitivity

We next tested our hypothesis that mice lacking adipose mTORC2 would be resistant to the metabolic benefits of CR by placing 10-week-old wild-type (WT) and AQ-RKO mice of both sexes on either *ad libitum* (AL) or CR diets. After 8 weeks, which is sufficient for CR to promote glucose tolerance and insulin sensitivity in C57BL/6J mice (Solon-Biet et al., 2015), we assessed the effects of CR on metabolic phenotypes. Both AQ-RKO mice and their WT littermates fed a CR diet had improved glucose tolerance compared to their AL-fed counterparts (Figures 2A and 2B). However, the improvement of insulin sensitivity induced by CR feeding that we observed in both male and female WT mice was completely blocked by deletion of adipose *Rictor* (Figures 2C, 2D, S1A, and S1B). In accordance with these results, we observed increased phosphorylation of AKT T308 and S473 in the adipose tissue of WT CR-fed mice relative to their WT AL-fed littermates following either acute stimulation by insulin or prolonged stimulation by refeeding, while in the absence of adipose *Rictor*, CR had no effect on the phosphorylation of AKT in adipose tissue in response to these stimuli (Figures S1C–S1F, S2A, and S2B). In contrast, we observed no effect of genotype on AKT phosphorylation in skeletal muscle (Figures S2C and S2D).

Consistent with the improved glucose tolerance of both genotypes of mice on a CR diet and previous reports of fasting hyperinsulinemia in mice lacking adipose *Rictor* (Tang et al., 2016; Cybulski et al., 2009), we observed hyperinsulinemia following refeeding in AQ-RKO mice of both sexes fed either AL or CR; curiously, CR potentiated the hyperinsulinemia we observed in AL-fed mice (Figures 2E and 2F). Consistent with the above results, we found that CR improved pyruvate tolerance equally well in both WT and AQ-RKO mice, indicating effective suppression of hepatic gluconeogenesis by insulin (Figure 2G). In accordance with these results, we observed no effect of genotype on AKT phosphorylation in the liver (Figures S2E and S2F).

Loss of Adipose *Rictor* Impairs the Metabolic Adaptation to a CR Diet

The effects of CR on insulin sensitivity likely result in part from reduced adiposity. In addition, CR substantially alters whole-body lipid metabolism, in part by reprogramming WAT; CR upregulates lipogenesis in WAT upon refeeding (Bruss et al., 2010), which may contribute to the beneficial effects of CR on systemic insulin sensitivity. We observed that the loss of

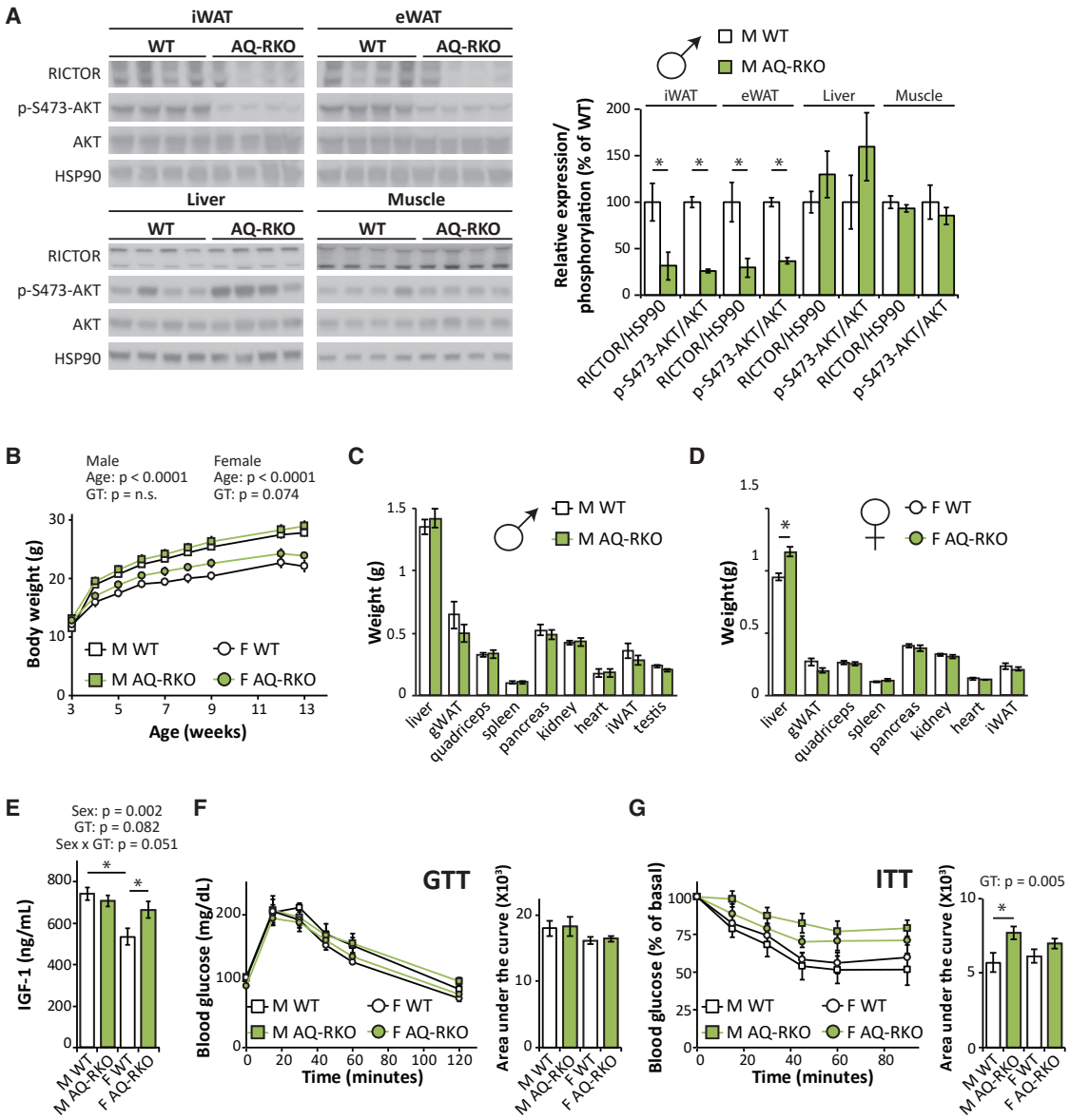

Figure 1. Mice Lacking Adipose mTORC2 Are Glucose Tolerant and Insulin Resistant

(A) Western blot analysis and quantification of RICTOR expression and mTORC2 activity in the iWAT, eWAT, liver, and muscle of AQ-RKO mice and their wild-type (WT) littermates (n = 4 per group, *p < 0.05, t test).

(B) Weights of male and female WT and AQ-RKO mice (n = 8–12 per group [males], n = 4 per group [females]; statistics for the overall effects of age, genotype [GT], and the interactions represent the p value from a repeated-measures two-way ANOVA conducted separately for each sex).

(C and D) Tissue weights of 20-week-old male (C) and female (D) WT and AQ-RKO mice (n = 5–9 per group, *p < 0.05, t test).

(E) Plasma IGF-1 of 22-week-old WT and AQ-RKO mice (n = 5 per group, statistics for the overall effects of sex, GT, and the interaction represent the p value from a two-way ANOVA; *p < 0.05, from a Holm-Sidak's post-test examining the effect of parameters identified as significant in the two-way ANOVA).

(F and G) Glucose (F) and (G) insulin tolerance of 10- to 12-week-old mice (n = 6–9 per group; for area under the curve [AUC], statistics for the overall effects of sex, GT, and the interaction represent the p value from a two-way ANOVA, *p < 0.05, from a Holm-Sidak's post-test examining the effect of parameters identified as significant in the two-way ANOVA).

Data are represented as mean ± SEM.

adipose mTORC2 did not substantially impact the effect of CR on adiposity; CR was equally effective at preventing the accretion of fat mass in both WT and AQ-RKO mice (Figures 3A and 3B). The body weight and lean mass of WT and AQ-RKO mice also responded similarly to CR (Figures 3C–3F). Thus, CR was equally effective at reducing adiposity in WT and AQ-RKO mice (Figures 3G and 3H).

We next examined the role of mTORC2 in the upregulation of lipogenesis by CR following refeeding. WT and AQ-RKO mice were placed in metabolic chambers, allowing us to assess

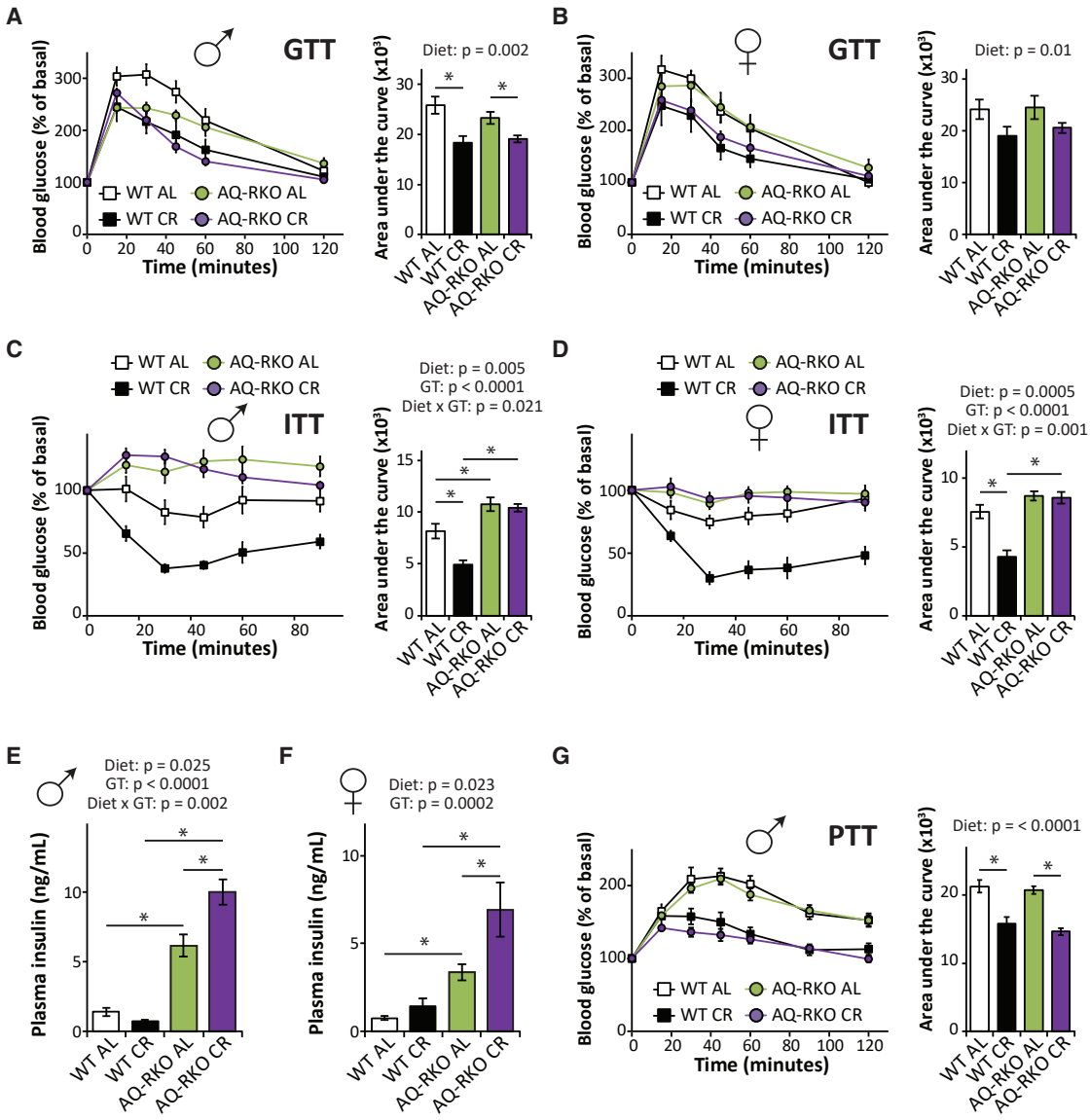

Figure 2. Adipose mTORC2 Is Required for the CR-Induced Increase in Insulin Sensitivity

(A and B) Glucose tolerance test of male (A) and female (B) WT and AQ-RKO mice after 9 weeks on indicated dietary regimens (n = 5–14 mice per group).
(C and D) Insulin tolerance test of male (C) and female (D) WT and AQ-RKO mice after 10 weeks on indicated dietary regimens (n = 9–19 mice per group).
(E and F) Plasma insulin in male (E) and female (F) mice after an overnight fast followed by refeeding for 3 h (n = 5–8 per group).
(G) Pyruvate tolerance test of male WT and AQ-RKO mice after 11 weeks on indicated dietary regimens (n = 14–19 per group).
Statistics for the overall effects of diet, GT, and the interaction represent the p value from a two-way ANOVA; *p < 0.05, from a Holm-Sidak's post-test examining the effect of parameters identified as significant in the two-way ANOVA. Data are represented as mean ± SEM.

substrate utilization by examining the respiratory exchange ratio (RER). RER is calculated using the ratio of O_2 consumed and CO_2 produced and approaches 1.0 when carbohydrates are being primarily utilized for energy production and approaches 0.7 when lipids are the predominant energy sources (Hasek et al., 2010). An RER >1.0 reflects the utilization of carbohydrates for active *de novo* lipogenesis (Bruss et al., 2010). Consistent with previous reports that CR-fed mice engage in rapid lipogenesis following refeeding and sustain themselves the rest of the day via the utilization of these stored lipids (Bruss et al., 2010), we observed that RER rapidly rose above 1.0 in WT CR mice following refeeding and ~6 h later fell below 0.8 (Figures 4A and 4B). In contrast, AQ-RKO CR-fed mice of both sexes had a blunted lipogenic response to refeeding, and AQ-RKO CR male mice had an intermediate RER for the majority of the dark cycle, suggesting that these animals relied on a mix of carbohydrate and lipid stores (Figures 4A and 4B).

To verify our model that AQ-RKO mice fed a CR diet had a reduced ability to induce lipogenesis following refeeding, we sacrificed mice 3 h after refeeding and examined lipogenic

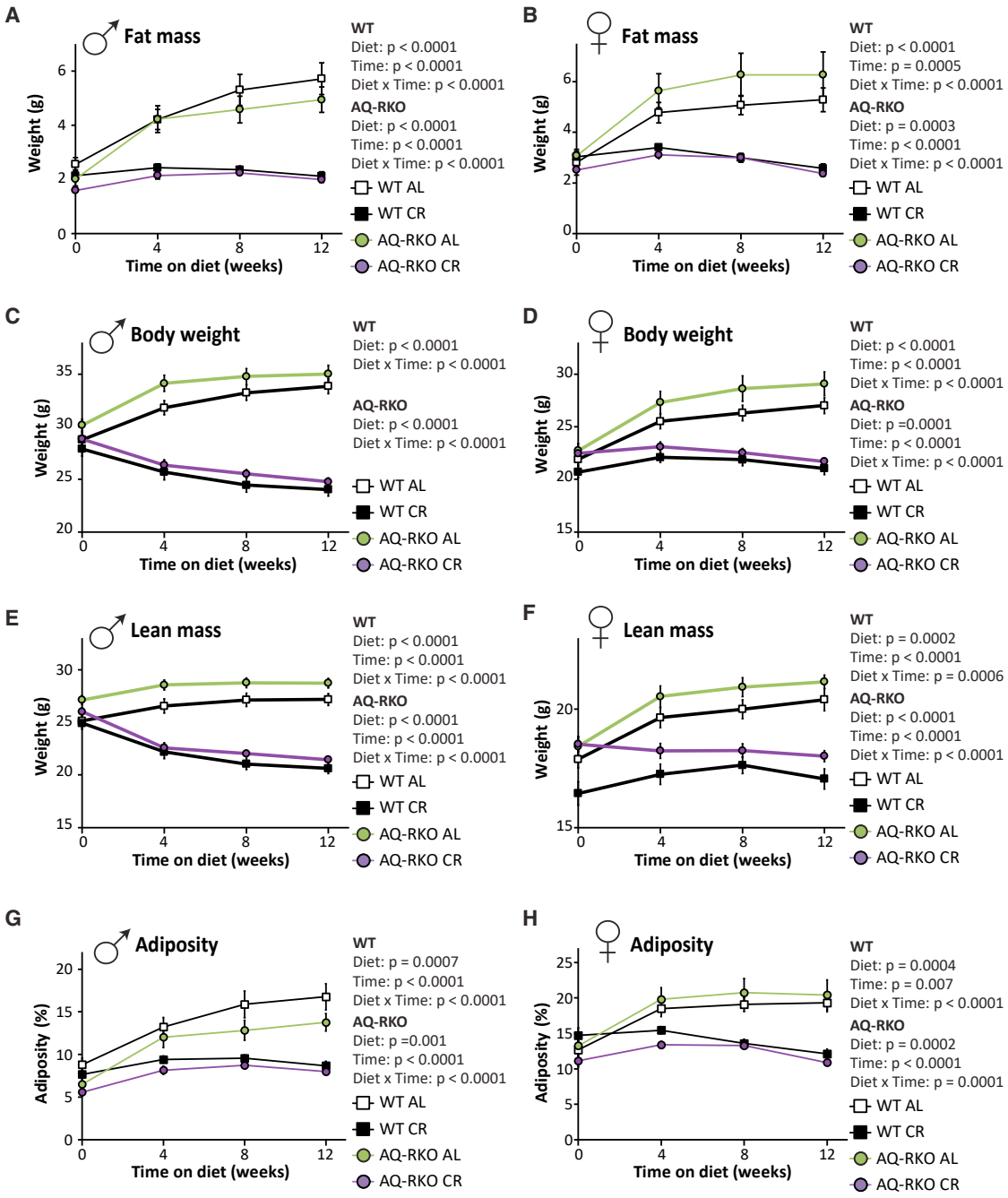

Figure 3. Loss of Adipose mTORC2 Does Not Affect the Response of Body Composition to CR

Fat mass, weight, lean mass, and adiposity of male (A, C, E, and G) and female (B, D, F, and H) WT and AQ-RKO mice fed either AL or CR diets starting at 10 weeks of age (n = 12–16 per group; statistics for the overall effects of diet, GT, and the interaction represent the p value from a repeated-measures two-way ANOVA conducted separately for each GT). Data are represented as mean ± SEM.

gene expression in iWAT. In agreement with our RER data, we observed that CR robustly induced the expression of many genes required for *de novo* lipogenesis, including ATP-citrate lyase (*Acly*), acetyl-CoA carboxylase (*Acc*), fatty acid synthase (*Fasn*), and elongation of very-long-chain fatty acids 6 (*Elovl6*), in WT mice (Figures 4C and 4D). However, CR had a substantially weaker impact on the expression of these lipogenic genes in AQ-RKO mice (Figures 4C and 4D).

De novo lipogenesis is regulated by several transcriptional factors, including carbohydrate-responsive element-binding proteins (ChREBPs) (Uyeda and Repa, 2006) and sterol regulatory element-binding proteins (SREBPs) (Horton et al., 2002).

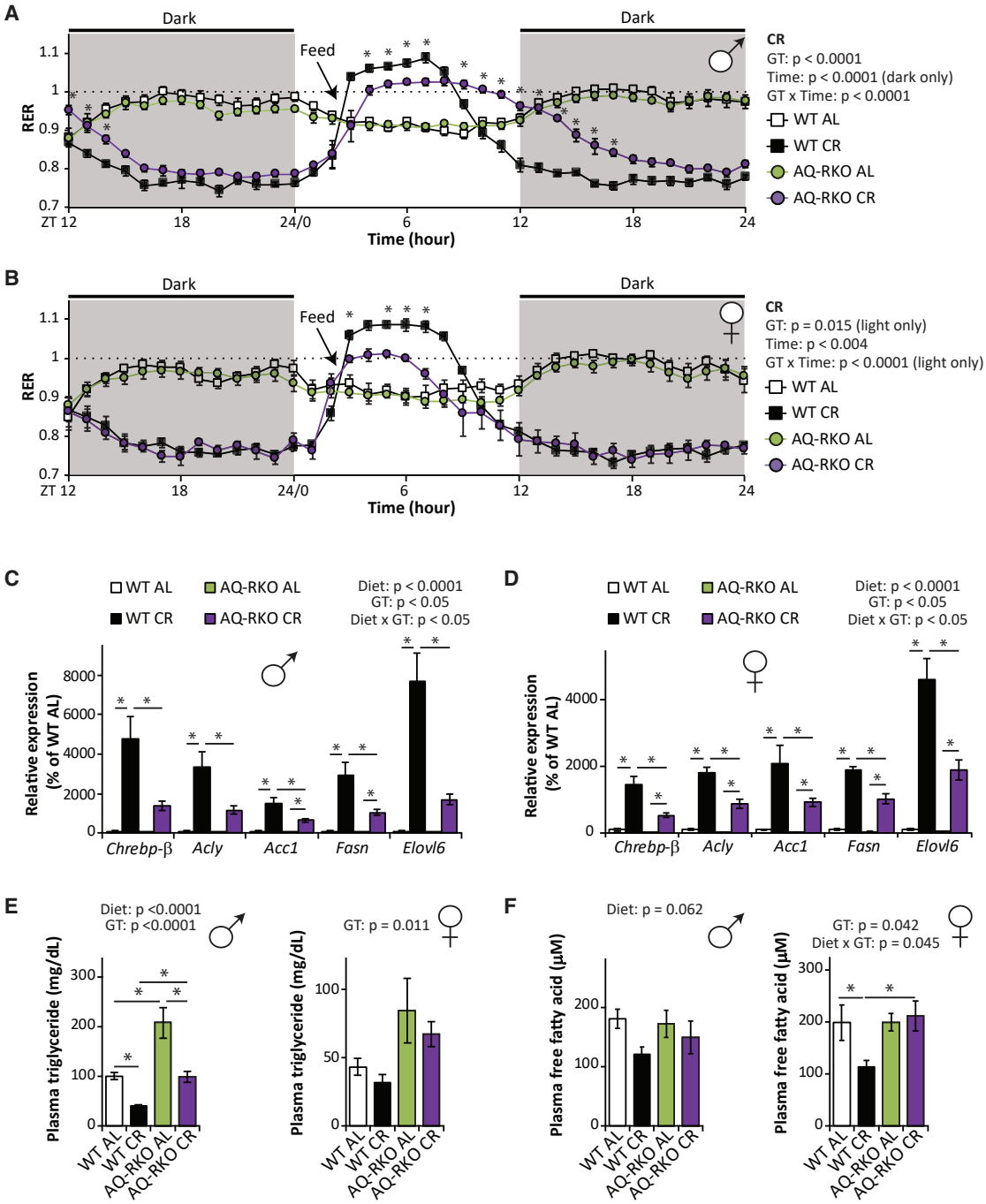

Figure 4. Loss of Adipose mTORC2 Attenuates CR-Mediated Reprogramming of Adipose Lipid Metabolism

(A and B) Respiratory exchange ratio (RER) of male (A) and female (B) WT and AQ-RKO mice after 7-week AL or CR regimens (n = 4–12 per group; statistics for the overall effects of GT, time, and the interaction represent the p value from a repeated-measures two-way ANOVA conducted on WT CR and AQ-RKO CR mice; *p < 0.05, from a Holm-Sidak's post-test; dark (shaded) and light phases were analyzed separately).

(C and D) Expression of *Chrebp-β* and related lipogenic genes in the iWAT of male (C) and female (D) WT and AQ-RKO mice after 12 weeks on the indicated diets (n = 6 per group; statistics for the overall effects of diet, GT, and the interaction represent the p value from a two-way ANOVA for each gene; *p < 0.05, from Holm-Sidak's post-tests conducted for the effect of diet and GT).

(E and F) Plasma triglycerides (E) and free fatty acids (F) in WT and AQ-RKO mice after 12 weeks on the indicated diets (n = 5–8 per group; statistics for the overall effects of diet, GT, and the interaction represent the p value from a two-way ANOVA conducted separately for each sex; * = p < 0.05, from Holm-Sidak's post-tests conducted for the effect of diet and GT).

Data are represented as mean ± SEM.

In agreement with a recent report implicating adipose mTORC2 in the control of ChREBP-β-dependent *de novo* lipogenesis (Tang et al., 2016), we observed that CR induced *Chrebp-β* strongly in the iWAT of CR-fed WT mice, but to a much lesser degree in mice lacking adipose mTORC2 (Figures 4C and 4D). Other transcriptional factors important for lipogenesis in adipose tissue such as *Chrebp-a* and *Srebp1-c* were also downregulated in AL-fed AQ-RKO mice; however, deletion of adipose *Rictor* attenuated the ability of CR to upregulate these transcriptional factors only in females (Figure S3A). While adipose tissue is the major site of lipogenesis in CR-fed mice (Bruss et al., 2010), the liver is also an important site for *de novo* lipogenesis. To assess possible indirect effects of adipose *Rictor* deletion on hepatic lipogenesis, we examined the expression of a panel of key lipogenic genes in this tissue. Although CR robustly increased the expression of almost of all these genes, we observed no effect of genotype on lipogenic gene expression on either AL or CR diets (Figure S3B).

CR activates thermogenesis as a mechanism to defend body temperature (Fabbiano et al., 2016). We found that WT males, but not WT females, fed a CR diet had increased expression of uncoupled protein 1 (*Ucp1*) mRNA as well as increased expression of UCP1 protein in the iWAT; however, neither male nor female AQ-RKO mice had increased expression of UCP1 at either the mRNA or protein level in response to CR (Figures S3C–S3F). The expression of two other key thermogenic genes, cell-death-inducing DNA fragmentation factor alpha-like effector A (*Cidea*) and elongation of very-long-chain fatty acids protein 3 (*Elovl3*), were significantly upregulated by CR in the iWAT of WT mice of both sexes but were not induced by CR in AQ-RKO mice (Figures S3C and S3D). Despite these significant differences at the molecular level, the morphology of iWAT from WT and AQ-RKO mice on either diet was very similar (Figure S4A). Furthermore, CR similarly remodeled the brown adipose tissue (BAT) of both WT and AQ-RKO mice (Figure S4B) at the histological level. As in the iWAT, the expression of UCP1 was increased by CR in the BAT of WT male mice, but not in AQ-RKO mice (Figure S4C).

We reasoned that as adipose *Rictor* deletion impacts the effects of CR on both substrate utilization and adipose lipogenesis, AQ-RKO mice might have altered levels of circulating lipids following refeeding. We observed that loss of adipose *Rictor* increased circulating levels of triglycerides in both males and females, irrespective of diet, and CR significantly reduced the plasma triglycerides levels of both WT and AQ-RKO males (Figure 4E). Plasma free fatty acids were significantly decreased by CR in female WT mice, but not in female AQ-RKO mice; in males, plasma free fatty acids were not significantly affected by genotype, but a CR diet showed a strong trend toward a decrease in plasma free fatty acids (Figure 4F). Furthermore, female AQ-RKO mice placed on a CR diet had significantly higher plasma cholesterol than WT CR-fed females (Figure S4D). Finally, we assessed lipid deposition in the liver and muscle by histology and found that CR promoted a similar reduction in lipid content in the liver of both WT and AQ-RKO mice and that no group had significant lipid deposition in the muscle (Figures S4E and S4F).

Longitudinal Assessment of the Role of Adipose mTORC2 in Body Composition and Glucose Homeostasis

The importance of adipose mTORC2 in the metabolic response to CR suggested to us that adipose mTORC2 might play a key role in regulating the many health benefits of long-term CR. To test this, we initiated a survival study in which 10-week-old WT and AQ-RKO mice were placed on either AL or CR diets; we then longitudinally assessed the effects of CR on weight and body composition, glycemic control, healthspan, and lifespan.

As we anticipated, both WT and AQ-RKO mice of either sex fed a CR diet weighed substantially less than AL-fed mice throughout their life (Figures S5A and S5B) and were leaner, with reduced levels of both fat and lean mass (Figures 5A–5D). However, we did observe significant differences in the body composition of AL-fed mice with age; in particular, male AQ-RKO AL-fed mice had significantly less fat mass than their WT littermates, particularly at 12 and 18 months of age (Figure 5A). Both male and female AL-fed AQ-RKO mice had greater lean mass throughout life than their AL-fed WT littermates, an effect that was statistically significant in females from 6 to 18 months of age (Figures 5C and 5D). The overall effect of *Rictor* loss was reduced adiposity over the course of the lifespan for AL-fed males, but not for AL-fed females (Figures 5E and 5F).

During the course of the study, we assessed glucose homeostasis as the mice aged. In agreement with our initial findings and studies conducted by Tang and colleagues in young mice (Tang et al., 2016), we found that AQ-RKO mice fed an AL diet had normal glucose tolerance even at advanced ages; indeed, there was a trend toward improved glucose tolerance of 8-month-old AQ-RKO male mice relative to the their WT littermates (Figures S5C–S5F). This glucose tolerance was observed despite the lifelong insulin resistance of AQ-RKO mice of both sexes relative to their WT littermates (Figures 6A–6D). Consistent with these results and previous reports (Tang et al., 2016), we observed increased fasting hyperinsulinemia and hypersecretion of insulin in response to glucose stimulation in AL-fed AQ-RKO mice (Figures S5G and S5H).

As we observed in our short-term study, while WT mice placed on a CR diet showed significantly improved insulin sensitivity at 9 months of age relative to WT AL-fed mice, a CR diet did not improve the insulin sensitivity of AQ-RKO mice at this age (Figures 6A, 6B, S6A, and S6B). At 2 years of age, although CR improved the insulin sensitivity of AQ-RKO mice relative to AL-fed mice of the same genotype, CR-fed AQ-RKO mice remained significantly more insulin resistant than CR-fed WT mice (Figures 6C, 6D, S6C, and S6D). Critically, at no age were AQ-RKO mice fed a CR diet more insulin sensitive than age-matched WT AL-fed mice.

Adipose mTORC2 Does Not Mediate the Effects of a CR Diet on Fitness and Longevity

Mice and humans become increasingly frail with age, and starting at 18 months of age, we utilized a recently validated mouse frailty index that permits the quantification of frailty by tracking the accumulation of deficits with age to assess the impact of CR on fitness in both genotypes (Kane et al., 2016; Rockwood et al., 2017; Whitehead et al., 2014). As we anticipated, we found

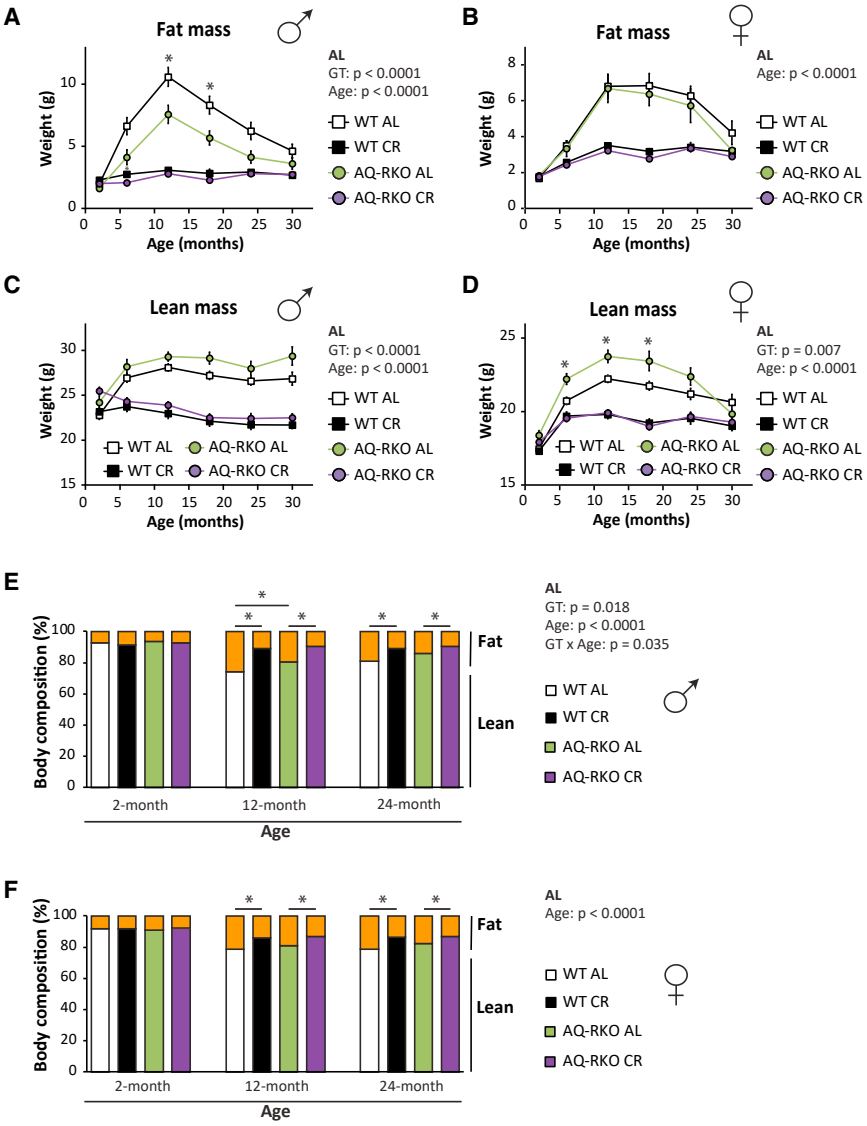

Figure 5. Longitudinal Assessment of Body Composition of WT and AQ-RKO Mice Fed AL or CR Diet

Longitudinal body composition analysis of WT and AQ-RKO mice.

(A and B) Fat mass of male (A) and female (B) mice.

(C and D) Lean mass of male (C) and female (D) mice.

(A–D) Numbers vary month by month; maximum n = 24–39 per group.

(E and F) Percentage of body fat mass and lean mass of male (E) and female (F) mice at 2, 12, and 24 months of age (n = 13–28 mice per group).

Statistics for the overall effects of GT, age, and the interaction represent the p value from a repeated-measures two-way ANOVA conducted for AL fed mice; *p < 0.05, from Holm-Sidak's post-test comparing WT and AQ-RKO AL-fed mice at each age. Data are represented as mean ± SEM.

that WT CR-fed male and female mice were significantly less frail than WT AL-fed mice of the same age and sex (Figures 7A and 7B). Surprisingly, we observed that the frailty of AQ-RKO AL-fed mice and WT AL-fed mice was similar and that the fitness of both male and female AQ-RKO mice was improved by a CR diet to the same extent as CR improved the fitness of WT mice (Figures 7A and 7B).

Finally, we determined the effect of adipose *Rictor* deletion on longevity and the response to CR. In contrast to our previously reported observation of a sharp, male-specific decrease in the lifespan of mice lacking hepatic *Rictor* (Lamming et al., 2014b), we find that loss of adipose mTORC2 signaling has no significant effect on male lifespan; instead, we find a 7% decrease in median female lifespan (Figures 7C–7E). As expected, a CR diet significantly extended the lifespan of both male and female WT mice. Surprisingly, but consistent with our frailty findings, we found that a CR diet robustly extends the lifespan of both male and female AQ-RKO mice; indeed, the lifespan of AQ-RKO mice fed a CR diet was indistinguishable from that of their WT littermates (Figures 7C–7E).

DISCUSSION

Despite thorough investigation over the last century, the physiological and molecular mechanisms underlying the benefits of CR on healthspan and longevity have remained elusive. One of the most widely conserved effects of CR in mammals is improved insulin sensitivity (Lamming and Anderson, 2014). Given the well-known association of insulin resistance with obesity, diabetes, cardiovascular disease, Alzheimer's disease, and other diseases of aging, it is conceptually appealing to posit that insulin sensitivity mediates the beneficial effects of a CR diet (Evans and Goldfine, 2013; Williamson et al., 2012; Fontana and Partridge, 2015). Although this hypothesis has never been directly tested, the extended longevity of a mouse model of whole-body insulin resistance (*Irs1*$^{-/-}$; Selman et al., 2008) and other genetic or pharmaceutical mouse models in which insulin resistance has been induced in one or more tissues suggested to us that this hypothesis was incorrect or incomplete.

Here, we have directly tested the hypothesis that the beneficial effects of CR are mediated by improved insulin sensitivity using AQ-RKO mice. These mice, which in our hands have lifelong insulin resistance and fasting hyperinsulinemia when fed AL, remain glucose tolerant due to increased glucose-stimulated insulin secretion. The frailty and longevity of AQ-RKO mice of both sexes on an AL diet is similar to that of their WT littermates, with reduced lifespan only in female AQ-RKO mice. Finally, we have found that AQ-RKO mice have an impaired metabolic response to CR, resisting CR-induced improvements in insulin

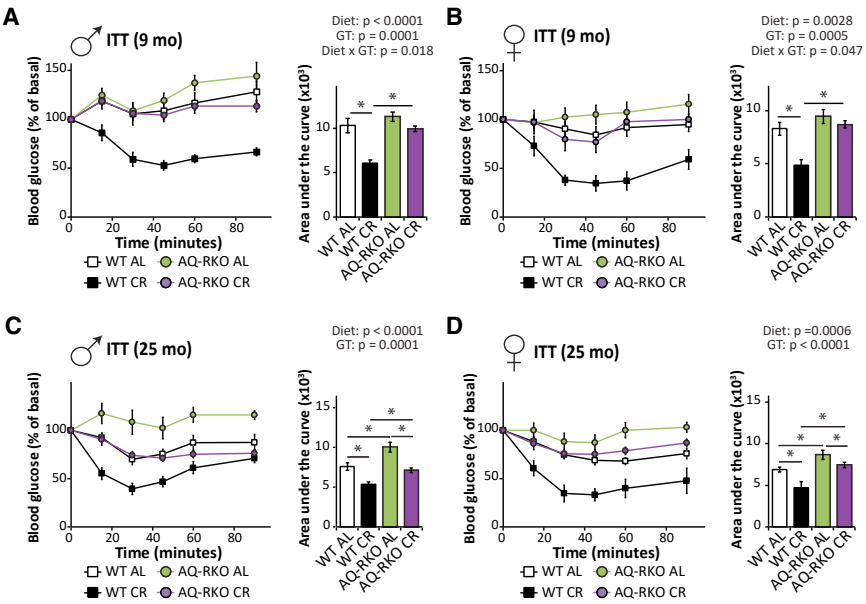

Figure 6. Deletion of Adipose *Rictor* Blocks Calorie Restriction from Improving Organismal Insulin Sensitivity

Insulin tolerance tests of 9-month-old male (A) and female (B) WT and AQ-RKO mice as well as 25 month-old male (C) and female (D) WT and AQ-RKO mice. n = 6–13 per group; statistics for the overall effects of diet, GT, and the interaction represent the p value from a two-way ANOVA for each measurement; *p < 0.05, Tukey post-test. Data are represented as mean ± SEM.

sensitivity. This combination of phenotypes has enabled us to test the theory that the beneficial effects of a CR diet are mediated by improved insulin sensitivity. We find that despite the impaired metabolic response of AQ-RKO mice to a CR diet, AQ-RKO mice benefit fully from the effects of a CR diet with respect to both fitness and longevity. We conclude that although CR improves systemic insulin sensitivity, this improvement is not required for the beneficial effects of a CR diet on healthspan and lifespan (Figure 7F).

The question of what mediates the benefits of a CR diet on fitness and longevity remains open. While our results clearly demonstrate that improved insulin sensitivity is not required for CR to extend lifespan in C57BL/6J mice, numerous studies have found that interventions that promote insulin sensitivity do extend lifespan (e.g., Garratt et al., 2017; Templeman et al., 2017). Although a CR diet protects against tumors and carcinogenesis (Kalaany and Sabatini, 2009), an effect that would likely extend the lifespan of tumor-prone C57BL/6J mice, a study conducted over a decade ago found that a CR diet robustly extended the lifespan of mice lacking NF-E2-related factor 2 (Nrf2), despite being unable to suppress tumorigenesis (Pearson et al., 2008). As we have outlined in Figure 7F, while insulin sensitivity and cancer protection are both induced by a CR diet, neither effect is solely responsible for the effects of CR on the fitness and longevity of rodents. Future research into the mediators of CR may benefit from taking a similar approach to our study and that conducted by Pearson, in which the healthspan and lifespan of mouse models with a reduced response to specific facets of CR is investigated. The model we have developed here may be useful for testing whether improved insulin sensitivity mediates the extended health and longevity of a number of pharmaceutical interventions and genetic mouse models (Templeman et al., 2017; Garratt et al., 2017; Harrison et al., 2019; Strong et al., 2016).

An important limitation of our results is that here, we have primarily focused on systemic insulin sensitivity as measured by the acute clearance of glucose in response to an intraperitoneal injection of insulin, and we have not directly assessed many other aspects of insulin resistance or insulin action at different timescales. While we have not directly assessed tissue glucose uptake, the findings of Tang et al. (2016), our insulin tolerance test results, and our molecular data showing that CR-fed mice have increased insulin/PI3K signaling in iWAT following either acute insulin stimulation or refeeding suggest that the insulin resistance of AQ-RKO mice fed either an AL or CR diet is primarily mediated by reduced glucose uptake into adipose tissue. However, there may also be non-cell-autonomous effects of adipose *Rictor* deletion mediated by the reduced lipogenesis in AQ-RKO mice fed a CR diet. ChREBP-mediated lipogenesis in adipose tissue promotes systemic insulin sensitivity (Vijayakumar et al., 2017; Yore et al., 2014; Herman et al., 2012); thus, the impaired lipogenic response of AQ-RKO mice to a CR diet may blunt the effects of CR on the insulin sensitivity of other tissues. While we did not conduct a comprehensive examination of hormones and factors that might be altered in AQ-RKO mice and regulate insulin sensitivity, Tang and colleagues have reported that AQ-RKO mice have normal levels of tumor necrosis factor alpha (TNF-α), leptin, and resistin, with changes in adiponectin that are insufficient to explain the insulin resistance of AQ-RKO mice (Tang et al., 2016). Although we did not observe an effect of adipose *Rictor* loss on insulin/PI3K signaling in skeletal muscle or liver tissue, our examination of these tissues was limited, and the insulin sensitivity of these or other non-adipose tissues could be improved by a CR diet, even in AQ-RKO mice, and could therefore potentially contribute to, or even drive, the beneficial effects of CR on fitness and lifespan. While distinguishing between these possibilities will require further detailed investigation, we consider the latter hypothesis unlikely; in agreement with other groups, we find that loss of adipose mTORC2 results in hyperinsulinemia (Cybulski et al., 2009; Tang et al., 2016), and as we report here, even on a CR diet, AQ-RKO mice have relatively high levels of insulin. High insulin sensitivity in the context of hyperinsulinemia would result in increased signaling through the PI3K/AKT/mTORC1 signaling pathway, which would likely have deleterious rather than beneficial effects on health and

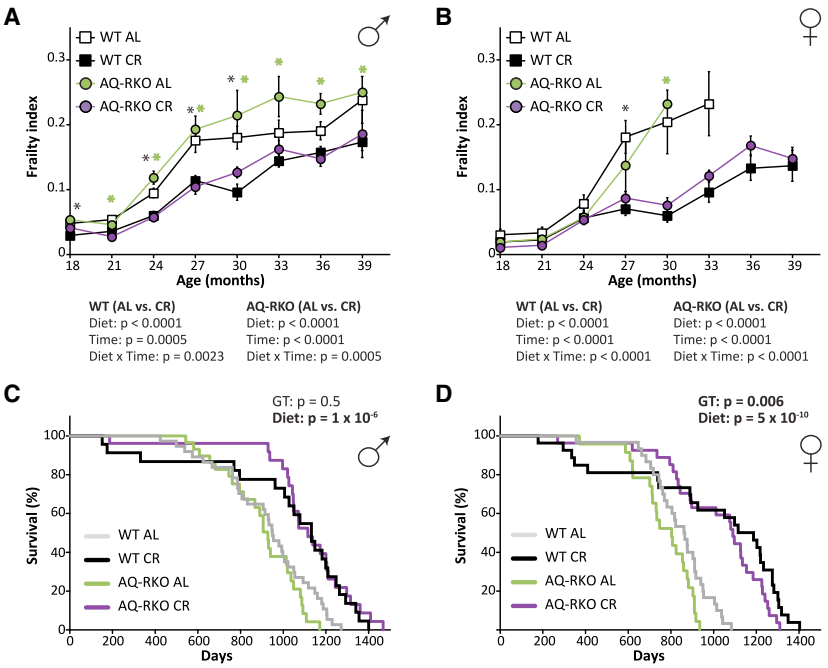

Figure 7. Adipose mTORC2 Is Dispensable for the Effects of CR on Healthspan and Lifespan

(A and B) Frailty of male (A) and female (B) WT and AQ-RKO mice (numbers vary month by month; maximum n = 20–37 per group). Statistics for the overall effects of diet, age, and the interaction represent the p value from a mixed-effects model (restricted maximum likelihood [REML]) conducted separately for each GT; * $p < 0.05$ (black), Holm-Sidak's post-test comparing WT AL and WT CR-fed mice at each age; * $p < 0.05$ (green), Holm-Sidak's post-test comparing AQ-RKO AL and AQ-RKO CR-fed mice at each age.

(C and D) Kaplan-Meier plots showing the lifespan of male (C) and female (D) WT and AQ-RKO mice. For each sex, the two-tailed stratified log-rank p value for the effect of GT and diet is indicated.

(E) Median lifespans for the survival curves plotted in (C) and (D) and the individual log-rank p values for the indicated pairwise comparisons.

(F) CR effects on fitness and longevity are independent from its effects on insulin sensitivity and cancer.

Data are represented as mean ± SEM.

E

Males	Median survival	Comparison of male ls	Δ (%)	p (log rank)
WT AL	949	WT AL vs AQ-RKO AL	-2.21	0.1427
WT CR	1132	WT CR vs AQ-RKO CR	-1.50	0.5102
AQ-RKO AL	928	WT AL vs WT CR	19.28	0.0044
AQ-RKO CR	1115	AQ-RKO AL vs AQ-RKO CR	20.15	<0.0001

Females	Median survival	Comparison of female ls	Δ (%)	p (log rank)
WT AL	863	WT AL vs AQ-RKO AL	-6.95	0.0146
WT CR	1187	WT CR vs AQ-RKO CR	-8.17	0.1279
AQ-RKO AL	803	WT AL vs WT CR	37.54	<0.0001
AQ-RKO CR	1090	AQ-RKO AL vs AQ-RKO CR	35.74	<0.0001

F

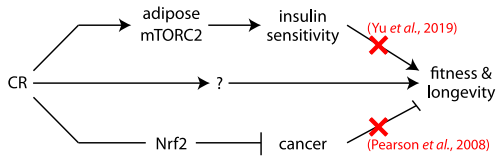

longevity (Blagosklonny, 2012; Dumas and Lamming, 2019; Lamming, 2014).

Rapamycin treatment extends the lifespan of mice (reviewed in Arriola Apelo and Lamming, 2016). The effects of rapamycin on health and longevity were originally believed to result from inhibition of mTORC1, but we and other groups have demonstrated that rapamycin also inhibits mTORC2 *in vivo* in multiple tissues, including liver and WAT (Lamming et al., 2012; Schreiber et al., 2015). Inhibition of hepatic mTORC2 by rapamycin results in hepatic insulin resistance, and it is now thought that many side effects of rapamycin may be driven by mTORC2 inhibition (Kennedy and Lamming, 2016). However, this does not eliminate the possibility that inhibition of mTORC2 may also have some benefits with respect to longevity, and indeed, mice heterozygous for the mTORC2 substrate *Akt1* have increased lifespan (Nojima et al., 2013). Thus, understanding both the positive and negative roles of mTORC2 in different tissues on health and longevity is of high importance as rapamycin and related compounds enter human clinical trials for diseases of aging (Mannick et al., 2014; Mannick et al., 2018; Kraig et al., 2018).

We have previously shown that diminishing mTORC2 activity specifically in the liver or in the whole body reduces male lifespan by at least 30% (Lamming et al., 2014b), while deletion of *Rictor* specifically in the hypothalamus reduces male lifespan by 10% and increases frailty in both sexes (Chellappa et al., 2019). Fitness was also reduced when *Rictor* was inducibly deleted in adult mice, which resulted in a progeroid phenotype. In contrast, we find that mTORC2 inhibition in adipose tissue has minimal effects on the fitness of either male or female mice, and specifically reduces median female lifespan by 7%, possibly as a consequence of elevated IGF-1 levels in *ad-libitum*-fed female mice. As loss of adipose mTORC2 signaling also significantly increases plasma triglycerides, these results suggest that inhibition of adipose mTORC2 signaling should be avoided when designing rapalog-based approaches to diseases of aging (Schreiber et al., 2019). Finally, we note that the induction of insulin resistance in adipose tissue did not result in the extended longevity observed in the FIRKO mouse (Blüher et al., 2003). Possible explanations for the difference include the degree of insulin resistance induced and the different Cre driver utilized by Bluher and colleagues. While we and others have hypothesized that insulin resistance may promote longevity in part by decreasing mTORC1 signaling (Blagosklonny, 2012; Lamming, 2014), and mTORC1 plays an important role in the regulation of thermogenesis (Tran et al., 2016), we did not observe altered mTORC1 signaling in mice lacking adipose *Rictor*.

In summary, we have tested the long-standing hypothesis that the beneficial effects of CR on health and longevity are the result of the CR-induced improvements in insulin sensitivity observed in both rodents and humans placed on a CR diet using a mouse model lacking adipose mTORC2 activity. We have determined that adipose mTORC2 has an essential role in the regulation of body composition and the survival of female mice fed AL. Further, adipose mTORC2 plays a role in the metabolic adaptation to CR and is required for CR to improve insulin sensitivity. CR-induced improvements in insulin sensitivity are widely seen in mammals and were proposed to mediate the beneficial effects of CR on health and longevity. Here, we disprove this hypothesis by showing that the CR-induced improvements in organismal insulin sensitivity are not required for the beneficial effects of CR on fitness and lifespan. We suggest that the utilization of mouse strains with impaired responses to different aspects of CR may be a useful approach to identifying the true physiological and molecular mechanisms by which CR promotes mammalian health and longevity.

STAR★METHODS

Detailed methods are provided in the online version of this paper and include the following:

- KEY RESOURCES TABLE
- LEAD CONTACT AND MATERIALS AVAILABILITY
- EXPERIMENTAL MODEL AND SUBJECT DETAILS
- METHOD DETAILS
  - *In vivo* tests
  - Tissue harvest
  - Histology
  - Plasma hormone and lipid measurement
  - Quantitative PCR
  - Immunoblotting
  - Lifespan and necropsy
  - Frailty
- QUANTIFICATION AND STATISTICAL ANALYSIS
- DATA AND CODE AVAILABILITY

SUPPLEMENTAL INFORMATION

Supplemental Information can be found online at https://doi.org/10.1016/j.celrep.2019.08.084.

ACKNOWLEDGMENTS

We would like to thank all members of the Lamming lab, particularly Dr. Cara Green, for critical reading of the manuscript and our colleagues at UW-Madison and beyond for their thoughtful input. We thank A. Broman of the UW-Madison Department of Biostatistics & Medical Informatics for assistance with analysis of lifespan data and R, and Drs. Christine Patterson and Evan Rosen for the gift of Adipoq-Cre mice and advice on genotyping. We thank Dr. Abigail Radcliff and Kathy Krentz for assistance with rederivation. We thank Dr. Dena Cohen for advice regarding the implementation of CR, phenotyping of CR mice, and continual support and encouragement. The work was supported in part by the NIH National Institute on Aging (AG041765, AG050135, AG051974, AG056771, and AG062328 to D.W.L.), a Glenn Foundation Award for Research in the Biological Mechanisms of Aging to D.W.L., and startup funds from the University of Wisconsin-Madison School of Medicine and Public Health and Department of Medicine to D.W.L. This research was conducted while D.W.L. was an AFAR Research Grant recipient from the American Federation for Aging Research. D.Y. was supported in part by a fellowship from the American Heart Association (17PRE33410983). N.E.C. was supported by a training grant from the UW Institute on Aging (NIA T32 AG000213). The UW Carbone Cancer Center (UWCCC) Experimental Pathology Laboratory is supported by UWCCC support grant P30 CA014520 from the NIH National Cancer Institute. The project was supported by the Clinical and Translational Science Award (CTSA) program through the NIH National Center for Advancing Translational Sciences (NCATS) (grant UL1TR002373). The Lamming laboratory is supported in part by the U.S. Department of Veterans Affairs (I01-BX004031), and this work was supported using facilities and resources from the William S. Middleton Memorial Veterans Hospital. The content is solely the responsibility of the authors and does not necessarily represent the official views of the NIH. This work does not represent the views of the Department of Veterans Affairs or the United States Government.

AUTHOR CONTRIBUTIONS

D.Y. and D.W.L. conceived the experiments. D.W.L. secured funding. D.Y., J.L.T., S.E.Y., B.R.M., M.H.W., D.S.S., N.E.C., E.L.B., J.A.B., F.A.S., and D.W.L. performed the experiments. D.Y., D.S.S., E.L.B., and D.W.L. analyzed the data. D.Y. and D.W.L. wrote the manuscript.

DECLARATION OF INTERESTS

D.W.L. has received funding from, and is a scientific advisory board member of, Aeonian Pharmaceuticals, which seeks to develop novel, selective mTOR inhibitors for the treatment of various diseases.

Received: March 25, 2019
Revised: July 29, 2019
Accepted: August 27, 2019
Published: October 1, 2019

REFERENCES

Arriola Apelo, S.I., and Lamming, D.W. (2016). Rapamycin: an inhibitor of aging emerges from the soil of Easter Island. J. Gerontol. A Biol. Sci. Med. Sci. *71*, 841–849.

Arriola Apelo, S.I., Neuman, J.C., Baar, E.L., Syed, F.A., Cummings, N.E., Brar, H.K., Pumper, C.P., Kimple, M.E., and Lamming, D.W. (2016). Alternative rapamycin treatment regimens mitigate the impact of rapamycin on glucose homeostasis and the immune system. Aging Cell *15*, 28–38.

Baar, E.L., Carbajal, K.A., Ong, I.M., and Lamming, D.W. (2016). Sex- and tissue-specific changes in mTOR signaling with age in C57BL/6J mice. Aging Cell *15*, 155–166.

Balasubramanian, P., Howell, P.R., and Anderson, R.M. (2017). Aging and caloric restriction research: a biological perspective with translational potential. EBioMedicine *21*, 37–44.

Blagosklonny, M.V. (2012). Once again on rapamycin-induced insulin resistance and longevity: despite of or owing to. Aging (Albany N.Y.) *4*, 350–358.

Blüher, M., Kahn, B.B., and Kahn, C.R. (2003). Extended longevity in mice lacking the insulin receptor in adipose tissue. Science *299*, 572–574.

Bruss, M.D., Khambatta, C.F., Ruby, M.A., Aggarwal, I., and Hellerstein, M.K. (2010). Calorie restriction increases fatty acid synthesis and whole body fat oxidation rates. Am. J. Physiol. Endocrinol. Metab. *298*, E108–E116.

Chellappa, K., Brinkman, J.A., Mukherjee, S., Morrison, M., Alotaibi, M.I., Carbajal, K.A., Alhadeff, A.L., Perron, I.J., Yao, R., Purdy, C.S., et al. (2019). Hypothalamic mTORC2 is essential for metabolic health and longevity. Aging Cell *18*, e13014.

Chen, D., Bruno, J., Easlon, E., Lin, S.J., Cheng, H.L., Alt, F.W., and Guarente, L. (2008). Tissue-specific regulation of SIRT1 by calorie restriction. Genes Dev. *22*, 1753–1757.

Cummings, N.E., Williams, E.M., Kasza, I., Konon, E.N., Schaid, M.D., Schmidt, B.A., Poudel, C., Sherman, D.S., Yu, D., Arriola Apelo, S.I., et al.

(2018). Restoration of metabolic health by decreased consumption of branched-chain amino acids. J. Physiol. *596*, 623–645.

Cybulski, N., Polak, P., Auwerx, J., Rüegg, M.A., and Hall, M.N. (2009). mTOR complex 2 in adipose tissue negatively controls whole-body growth. Proc. Natl. Acad. Sci. USA *106*, 9902–9907.

Dumas, S.N., and Lamming, D.W. (2019). Next generation strategies for geroprotection via mTORC1 inhibition. J. Gerontol. A Biol. Sci. Med. Sci., glz056.

Eguchi, J., Wang, X., Yu, S., Kershaw, E.E., Chiu, P.C., Dushay, J., Estall, J.L., Klein, U., Maratos-Flier, E., and Rosen, E.D. (2011). Transcriptional control of adipose lipid handling by IRF4. Cell Metab. *13*, 249–259.

Evans, J.L., and Goldfine, I.D. (2013). Aging and insulin resistance: just say iNOS. Diabetes *62*, 346–348.

Fabbiano, S., Suárez-Zamorano, N., Rigo, D., Veyrat-Durebex, C., Stevanovic Dokic, A., Colin, D.J., and Trajkovski, M. (2016). Caloric restriction leads to browning of white adipose tissue through type 2 immune signaling. Cell Metab. *24*, 434–446.

Fontana, L., and Partridge, L. (2015). Promoting health and longevity through diet: from model organisms to humans. Cell *161*, 106–118.

Garratt, M., Bower, B., Garcia, G.G., and Miller, R.A. (2017). Sex differences in lifespan extension with acarbose and 17-α estradiol: gonadal hormones underlie male-specific improvements in glucose tolerance and mTORC2 signaling. Aging Cell *16*, 1256–1266.

Guertin, D.A., Stevens, D.M., Thoreen, C.C., Burds, A.A., Kalaany, N.Y., Moffat, J., Brown, M., Fitzgerald, K.J., and Sabatini, D.M. (2006). Ablation in mice of the mTORC components raptor, rictor, or mLST8 reveals that mTORC2 is required for signaling to Akt-FOXO and PKCalpha, but not S6K1. Dev. Cell *11*, 859–871.

Hagiwara, A., Cornu, M., Cybulski, N., Polak, P., Betz, C., Trapani, F., Terracciano, L., Heim, M.H., Rüegg, M.A., and Hall, M.N. (2012). Hepatic mTORC2 activates glycolysis and lipogenesis through Akt, glucokinase, and SREBP1c. Cell Metab. *15*, 725–738.

Harrison, D.E., Strong, R., Alavez, S., Astle, C.M., DiGiovanni, J., Fernandez, E., Flurkey, K., Garratt, M., Gelfond, J.A.L., Javors, M.A., et al. (2019). Acarbose improves health and lifespan in aging HET3 mice. Aging Cell *18*, e12898.

Hasek, B.E., Stewart, L.K., Henagan, T.M., Boudreau, A., Lenard, N.R., Black, C., Shin, J., Huypens, P., Malloy, V.L., Plaisance, E.P., et al. (2010). Dietary methionine restriction enhances metabolic flexibility and increases uncoupled respiration in both fed and fasted states. Am. J. Physiol. Regul. Integr. Comp. Physiol. *299*, R728–R739.

Herman, M.A., Peroni, O.D., Villoria, J., Schön, M.R., Abumrad, N.A., Blüher, M., Klein, S., and Kahn, B.B. (2012). A novel ChREBP isoform in adipose tissue regulates systemic glucose metabolism. Nature *484*, 333–338.

Holzenberger, M., Dupont, J., Ducos, B., Leneuve, P., Géloën, A., Even, P.C., Cervera, P., and Le Bouc, Y. (2003). IGF-1 receptor regulates lifespan and resistance to oxidative stress in mice. Nature *421*, 182–187.

Horton, J.D., Goldstein, J.L., and Brown, M.S. (2002). SREBPs: activators of the complete program of cholesterol and fatty acid synthesis in the liver. J. Clin. Invest. *109*, 1125–1131.

Kalaany, N.Y., and Sabatini, D.M. (2009). Tumours with PI3K activation are resistant to dietary restriction. Nature *458*, 725–731.

Kane, A.E., Hilmer, S.N., Boyer, D., Gavin, K., Nines, D., Howlett, S.E., de Cabo, R., and Mitchell, S.J. (2016). Impact of longevity interventions on a validated mouse clinical frailty index. J. Gerontol. A Biol. Sci. Med. Sci. *71*, 333–339.

Kennedy, B.K., and Lamming, D.W. (2016). The mechanistic target of rapamycin: the grand conductor of metabolism and aging. Cell Metab. *23*, 990–1003.

Kenyon, C. (2001). A conserved regulatory system for aging. Cell *105*, 165–168.

Kleinert, M., Parker, B.L., Fritzen, A.M., Knudsen, J.R., Jensen, T.E., Kjøbsted, R., Sylow, L., Ruegg, M., James, D.E., and Richter, E.A. (2017). Mammalian target of rapamycin complex 2 regulates muscle glucose uptake during exercise in mice. J. Physiol. *595*, 4845–4855.

Kraig, E., Linehan, L.A., Liang, H., Romo, T.Q., Liu, Q., Wu, Y., Benavides, A.D., Curiel, T.J., Javors, M.A., Musi, N., et al. (2018). A randomized control trial to establish the feasibility and safety of rapamycin treatment in an older human cohort: immunological, physical performance, and cognitive effects. Exp. Gerontol. *105*, 53–69.

Kumar, A., Harris, T.E., Keller, S.R., Choi, K.M., Magnuson, M.A., and Lawrence, J.C., Jr. (2008). Muscle-specific deletion of rictor impairs insulin-stimulated glucose transport and enhances basal glycogen synthase activity. Mol. Cell. Biol. *28*, 61–70.

Kumar, A., Lawrence, J.C., Jr., Jung, D.Y., Ko, H.J., Keller, S.R., Kim, J.K., Magnuson, M.A., and Harris, T.E. (2010). Fat cell-specific ablation of rictor in mice impairs insulin-regulated fat cell and whole-body glucose and lipid metabolism. Diabetes *59*, 1397–1406.

Lamming, D.W. (2014). Diminished mTOR signaling: a common mode of action for endocrine longevity factors. Springerplus *3*, 735.

Lamming, D.W., and Anderson, R.M. (2014). Metabolic Effects of Caloric Restriction. (John Wiley & Sons).

Lamming, D.W., Ye, L., Katajisto, P., Goncalves, M.D., Saitoh, M., Stevens, D.M., Davis, J.G., Salmon, A.B., Richardson, A., Ahima, R.S., et al. (2012). Rapamycin-induced insulin resistance is mediated by mTORC2 loss and uncoupled from longevity. Science *335*, 1638–1643.

Lamming, D.W., Demirkan, G., Boylan, J.M., Mihaylova, M.M., Peng, T., Ferreira, J., Neretti, N., Salomon, A., Sabatini, D.M., and Gruppuso, P.A. (2014a). Hepatic signaling by the mechanistic target of rapamycin complex 2 (mTORC2). FASEB J. *28*, 300–315.

Lamming, D.W., Mihaylova, M.M., Katajisto, P., Baar, E.L., Yilmaz, O.H., Hutchins, A., Gultekin, Y., Gaither, R., and Sabatini, D.M. (2014b). Depletion of Rictor, an essential protein component of mTORC2, decreases male lifespan. Aging Cell *13*, 911–917.

Lee, K.Y., Russell, S.J., Ussar, S., Boucher, J., Vernochet, C., Mori, M.A., Smyth, G., Rourk, M., Cederquist, C., Rosen, E.D., et al. (2013). Lessons on conditional gene targeting in mouse adipose tissue. Diabetes *62*, 864–874.

Linnemann, A.K., Neuman, J.C., Battiola, T.J., Wisinski, J.A., Kimple, M.E., and Davis, D.B. (2015). Glucagon-like peptide-1 regulates cholecystokinin production in β-cells to protect from apoptosis. Mol. Endocrinol. *29*, 978–987.

López-Lluch, G., and Navas, P. (2016). Calorie restriction as an intervention in ageing. J. Physiol. *594*, 2043–2060.

Madeo, F., Carmona-Gutierrez, D., Hofer, S.J., and Kroemer, G. (2019). Caloric restriction mimetics against age-associated disease: targets, mechanisms, and therapeutic potential. Cell Metab. *29*, 592–610.

Mannick, J.B., Del Giudice, G., Lattanzi, M., Valiante, N.M., Praestgaard, J., Huang, B., Lonetto, M.A., Maecker, H.T., Kovarik, J., Carson, S., et al. (2014). mTOR inhibition improves immune function in the elderly. Sci. Transl. Med. *6*, 268ra179.

Mannick, J.B., Morris, M., Hockey, H.P., Roma, G., Beibel, M., Kulmatycki, K., Watkins, M., Shavlakadze, T., Zhou, W., Quinn, D., et al. (2018). TORC1 inhibition enhances immune function and reduces infections in the elderly. Sci. Transl. Med. *10*, eaaq1564.

Most, J., Tosti, V., Redman, L.M., and Fontana, L. (2017). Calorie restriction in humans: An update. Ageing Res. Rev. *39*, 36–45.

Nojima, A., Yamashita, M., Yoshida, Y., Shimizu, I., Ichimiya, H., Kamimura, N., Kobayashi, Y., Ohta, S., Ishii, N., and Minamino, T. (2013). Haploinsufficiency of akt1 prolongs the lifespan of mice. PLoS ONE *8*, e69178.

Pearson, K.J., Lewis, K.N., Price, N.L., Chang, J.W., Perez, E., Cascajo, M.V., Tamashiro, K.L., Poosala, S., Csiszar, A., Ungvari, Z., et al. (2008). Nrf2 mediates cancer protection but not prolongevity induced by caloric restriction. Proc. Natl. Acad. Sci. USA *105*, 2325–2330.

Rockwood, K., Blodgett, J.M., Theou, O., Sun, M.H., Feridooni, H.A., Mitnitski, A., Rose, R.A., Godin, J., Gregson, E., and Howlett, S.E. (2017). A frailty index based on deficit accumulation quantifies mortality risk in humans and in mice. Sci. Rep. *7*, 43068.

Rosen, E.D., and Spiegelman, B.M. (2006). Adipocytes as regulators of energy balance and glucose homeostasis. Nature *444*, 847–853.

Sarbassov, D.D., Guertin, D.A., Ali, S.M., and Sabatini, D.M. (2005). Phosphorylation and regulation of Akt/PKB by the rictor-mTOR complex. Science *307*, 1098–1101.

Schneider, C.A., Rasband, W.S., and Eliceiri, K.W. (2012). NIH Image to ImageJ: 25 years of image analysis. Nat. Methods *9*, 671–675.

Schreiber, K.H., Ortiz, D., Academia, E.C., Anies, A.C., Liao, C.Y., and Kennedy, B.K. (2015). Rapamycin-mediated mTORC2 inhibition is determined by the relative expression of FK506-binding proteins. Aging Cell *14*, 265–273.

Schreiber, K.H., Arriola Apelo, S.I., Yu, D., Brinkman, J.A., Velarde, M.C., Syed, F.A., Liao, C.Y., Baar, E.L., Carbajal, K.A., Sherman, D.S., et al. (2019). A novel rapamycin analog is highly selective for mTORC1 in vivo. Nat. Commun. *10*, 3194.

Selman, C., Lingard, S., Choudhury, A.I., Batterham, R.L., Claret, M., Clements, M., Ramadani, F., Okkenhaug, K., Schuster, E., Blanc, E., et al. (2008). Evidence for lifespan extension and delayed age-related biomarkers in insulin receptor substrate 1 null mice. FASEB J. *22*, 807–818.

Shiota, C., Woo, J.T., Lindner, J., Shelton, K.D., and Magnuson, M.A. (2006). Multiallelic disruption of the rictor gene in mice reveals that mTOR complex 2 is essential for fetal growth and viability. Dev. Cell *11*, 583–589.

Solon-Biet, S.M., Mitchell, S.J., Coogan, S.C., Cogger, V.C., Gokarn, R., McMahon, A.C., Raubenheimer, D., de Cabo, R., Simpson, S.J., and Le Couteur, D.G. (2015). Dietary protein to carbohydrate ratio and caloric restriction: comparing metabolic outcomes in mice. Cell Rep. *11*, 1529–1534.

Speakman, J.R., Mitchell, S.E., and Mazidi, M. (2016). Calories or protein? The effect of dietary restriction on lifespan in rodents is explained by calories alone. Exp. Gerontol. *86*, 28–38.

Strong, R., Miller, R.A., Antebi, A., Astle, C.M., Bogue, M., Denzel, M.S., Fernandez, E., Flurkey, K., Hamilton, K.L., Lamming, D.W., et al. (2016). Longer lifespan in male mice treated with a weakly estrogenic agonist, an antioxidant, an α-glucosidase inhibitor or a Nrf2-inducer. Aging Cell *15*, 872–884.

Therneau, T. (2015). A package for survival analysis in S, version 2.38. https://CRAN.R-project.org/package=survival.

Tang, Y., Wallace, M., Sanchez-Gurmaches, J., Hsiao, W.Y., Li, H., Lee, P.L., Vernia, S., Metallo, C.M., and Guertin, D.A. (2016). Adipose tissue mTORC2 regulates ChREBP-driven de novo lipogenesis and hepatic glucose metabolism. Nat. Commun. *7*, 11365.

Templeman, N.M., Flibotte, S., Chik, J.H.L., Sinha, S., Lim, G.E., Foster, L.J., Nislow, C., and Johnson, J.D. (2017). Reduced circulating insulin enhances insulin sensitivity in old mice and extends lifespan. Cell Rep. *20*, 451–463.

Tran, C.M., Mukherjee, S., Ye, L., Frederick, D.W., Kissig, M., Davis, J.G., Lamming, D.W., Seale, P., and Baur, J.A. (2016). Rapamycin blocks induction of the thermogenic program in white adipose tissue. Diabetes *65*, 927–941.

Uyeda, K., and Repa, J.J. (2006). Carbohydrate response element binding protein, ChREBP, a transcription factor coupling hepatic glucose utilization and lipid synthesis. Cell Metab. *4*, 107–110.

Vijayakumar, A., Aryal, P., Wen, J., Syed, I., Vazirani, R.P., Moraes-Vieira, P.M., Camporez, J.P., Gallop, M.R., Perry, R.J., Peroni, O.D., et al. (2017). Absence of carbohydrate response element binding protein in adipocytes causes systemic insulin resistance and impairs glucose transport. Cell Rep. *21*, 1021–1035.

Whitehead, J.C., Hildebrand, B.A., Sun, M., Rockwood, M.R., Rose, R.A., Rockwood, K., and Howlett, S.E. (2014). A clinical frailty index in aging mice: comparisons with frailty index data in humans. J. Gerontol. A Biol. Sci. Med. Sci. *69*, 621–632.

Williamson, R., McNeilly, A., and Sutherland, C. (2012). Insulin resistance in the brain: an old-age or new-age problem? Biochem. Pharmacol. *84*, 737–745.

Yilmaz, O.H., Katajisto, P., Lamming, D.W., Gültekin, Y., Bauer-Rowe, K.E., Sengupta, S., Birsoy, K., Dursun, A., Yilmaz, V.O., Selig, M., et al. (2012). mTORC1 in the Paneth cell niche couples intestinal stem-cell function to calorie intake. Nature *486*, 490–495.

Yore, M.M., Syed, I., Moraes-Vieira, P.M., Zhang, T., Herman, M.A., Homan, E.A., Patel, R.T., Lee, J., Chen, S., Peroni, O.D., et al. (2014). Discovery of a class of endogenous mammalian lipids with anti-diabetic and anti-inflammatory effects. Cell *159*, 318–332.

Yu, D., Yang, S.E., Miller, B.R., Wisinski, J.A., Sherman, D.S., Brinkman, J.A., Tomasiewicz, J.L., Cummings, N.E., Kimple, M.E., Cryns, V.L., and Lamming, D.W. (2018). Short-term methionine deprivation improves metabolic health via sexually dimorphic, mTORC1-independent mechanisms. FASEB J. *32*, 3471–3482.

Yuan, M., Pino, E., Wu, L., Kacergis, M., and Soukas, A.A. (2012). Identification of Akt-independent regulation of hepatic lipogenesis by mammalian target of rapamycin (mTOR) complex 2. J. Biol. Chem. *287*, 29579–29588.

STAR★METHODS

KEY RESOURCES TABLE

REAGENT or RESOURCE	SOURCE	IDENTIFIER
Antibodies		
Rabbit polyclonal anti-Rictor	Cell Signaling Technology	Cat# 2140; RRID:AB_2179961
Rabbit monoclonal anti-p-S473 Akt	Cell Signaling Technology	Cat# 4060; Clone D9E; RRID:AB_2315049
Rabbit monoclonal anti-p-T308 Akt	Cell Signaling Technology	Cat# 2965; Clone C31E5E; RRID:AB_2255933
Rabbit monoclonal anti-Akt	Cell Signaling Technology	Cat# 4691; Clone C67E7; RRID:AB_915783
Rabbit monoclonal anti-HSP90	Cell Signaling Technology	Cat# 4877; Clone C45G5; RRID:AB_2233307
Rabbit polyclonal anti-p-S240/244 S6 ribosomal protein	Cell Signaling Technology	Cat# 2215; RRID:AB_331682
Rabbit monoclonal anti-S6 ribosomal protein	Cell Signaling Technology	Cat#2217; Clone 5G10; RRID:AB_331355
Rabbit monoclonal anti-p-T37/S46 4EBP1	Cell Signaling Technology	Cat# 2855; Clone 236B4; RRID: AB_560835
Rabbit polyclonal anti-4EBP1	Cell Signaling Technology	Cat# 9452; RRID:AB_331692
Mouse monoclonal anti-p-Y1150/1151 IRβ	Santa Cruz Biotechnology	Cat# sc-81500; Clone 10C3; RRID:AB_1125642
Rabbit polyclonal anti-Ucp1	Abcam	Cat# ab10983; RRID:AB_2241462
Mouse monoclonal anti-β-actin	Sigma	Cat# A2228; Clone AC-74; RRID:AB_476697
Chemicals, Peptides, and Recombinant Proteins		
Human Insulin	Eli Lilly	NDC 0002-8215-17 (Humulin R U-100)
Critical Commercial Assays		
Mouse IGF-1 ELISA	Crystal Chem	Cat# 80574
Ultra-sensitive mouse insulin ELISA	Crystal Chem	Cat# 90080
Triglyceride colorimetric assay	Cayman Chemical	Cat# 10010303
Free fatty acid fluorometric assay	Cayman Chemical	Cat# 700310
Cholesterol liquicolor kit	Stanbio Laboratory	Cat# 1010225
Experimental Models: Organisms/Strains		
Mouse strain: C57BL/6J; *Rictor* $^{loxP/loxP}$	David Sabatini Lab (Whitehead Institute for Biomedical Research)	N/A
Mouse strain: C57BL/6J; *Adiponectin-Cre*	Evan Rosen Lab (Beth Israel Deaconess Medical Center and Harvard Medical School)	N/A
Mouse strain: C57BL/6J; *Adiponectin-Cre; Rictor* $^{loxP/loxP}$	Dudley Lamming Lab (University of Wisconsin-Madison)	N/A
Oligonucleotides		
Primers for genotyping: see Table S1	This paper	N/A
Primers for RT-PCR: see Table S1	This paper	N/A
Software and Algorithms		
Prism 8	GraphPad Software	N/A
ImageJ	Schneider et al., 2012	https://imagej.nih.gov/ij/
R (v. 3.6.0) survival package (v. 2.44)	Therneau, 2015	https://cran.r-project.org/web/packages/survival/index.html
Other		
Normal Chow	Purina	Cat# 5001
2 g pre-weighed rodent diet	Purina	Cat# 1816539
3 g pre-weighed rodent diet	Purina	Cat# 1816541

LEAD CONTACT AND MATERIALS AVAILABILITY

This study did not generate new unique reagents. Further information and requests for resources and reagents should be directed to and will be fulfilled by the Lead Contact, Dudley W. Lamming (dlamming@medicine.wisc.edu).

EXPERIMENTAL MODEL AND SUBJECT DETAILS

All procedures were performed in conformance with institutional guidelines and were approved by the Institutional Animal Care and Use Committee of the William S. Middleton Memorial Veterans Hospital (Madison, WI, USA). Adipose specific *Rictor* knockout mice (AQ-RKO) were generated by crossing mice with a conditional allele of *Rictor* (Shiota et al., 2006) on a C57BL/6J background that we have previously described (Lamming et al., 2014b) to mice expressing Cre recombinase under the control of the mouse *Adipoq* promoter ((Eguchi et al., 2011), gift of Drs. Christine Patterson and Evan Rosen). Mice were kept on a daily 12 h light/dark cycle and fed Purina lab chow diet 5001 (Purina Cat# 5001) until 10 weeks of age. At 10 weeks of age, littermates of the same sex were randomly assigned to either continue on an *ad libitum* (AL) regimen, or were placed on a CR regimen and fed using pre-weighed rodent diets tablets (Purina Cat# 1816539 and Cat# 1816541), with progressively increasing restriction over the course of 2 weeks, with a maximum level of restriction of 40%, as previously described (Yilmaz et al., 2012; Lamming et al., 2014b). Briefly, animals housed 1, 2, or 3 to cage were fed, respectively, 3, 5, or 6 g of pre-weighed rodent diet tablets per day; the food intake of each cage was adjusted when the number of animals in the cage was altered, e.g., due to age-related mortality. CR animals were typically fed in the morning at approximately 8AM. For short-term studies, 10-week-old mice were placed on AL and CR regimens for 12 weeks before sacrifice. Mice were housed in a specific-pathogen-free (SPF) mouse facility under a 12:12 h light/dark cycle with free access to food and water, except for CR mice and where noted in the procedures below. Animals were group housed in static microisolator cages, except when temporarily housed in an Oxymax/CLAMS metabolic chamber system (Columbus Instruments).

METHOD DETAILS

In vivo tests

For glucose and pyruvate tolerance tests, food was withheld at 5 pm from *ad libitum* fed animals for 16 hours, and mice were then injected intraperitoneally with glucose (1 g/kg) or pyruvate (2 g/kg) as described previously (Yu et al., 2018). The insulin tolerance test desribed in Figure 1 was performed by fasting mice at 5 pm and injecting 0.75 U/kg of insulin intraperitoneally around 9 am the next morning. As CR-fed WT mice are extremely insulin sensitive and this procedure leads to extremely low blood glucose values during an ITT, all other insulin tolerance tests (except for the ones performed in 25-month-old mice, Figures 6C, 6D, S6C, S6D) were performed by fasting mice at 6 am in the morning and then injecting 0.5 U/kg of insulin (0.5U/kg) intraperitoneally at 10 am. ITTs in 25 month-old mice were performed using 0.75 U/kg as the response of all groups of mice to 0.5 U/kg was limited. In all ITTs, WT CR-fed animals that experienced hypoglycemia and needed to be rescued by adminsitration of glucose were not included in the presented results. A Bayer Contour blood glucose meter and test strips were used to measure blood glucose. For body composition analysis, lean and fat mass were measured using an EchoMRI Body Composition Analyzer (EchoMRI^{TM}) according to the manufacturer's procedures. To assess RER and heat production, we utilized an Oxymax/CLAMS metabolic chamber system following the manufacturer's instructions (Columbus Instruments).

Tissue harvest

Mice used for the short-term study were sacrificed in either in the fasted state, refed state or insulin-stimulated state after 12 weeks of feeding AL or CR. Mice sacrificed in the fasted state were fasted overnight starting at 5 pm and then sacrificed between 9 and 11 am the next morning. Mice sacrificed in the refed state were fasted at 5 pm for overnight and food was provided to both AL and CR mice at 8 am the next morning; the mice were then sacrificed approximately 3 hours later. Mice sacrificed in the insulin-stimulated state were fasted overnight for approximately 16 hours starting at 5 pm and were then injected I.P. with 0.75 U/kg of insulin 15 min prior to sacrifice (Arriola Apelo et al., 2016). Following blood collection via submandibular bleeding, mice were euthanized and tissues including liver, white adipose tissue (WAT), muscle, and brown adipose tissue (BAT) were immediately dissected and frozen in liquid nitrogen for subsequent molecular analysis or preserved for histological analysis.

Histology

Samples of brown adipose tissue (BAT), white adipose tissue (WAT), liver, and muscle were isolated following sacrifice. BAT and WAT were fixed in 4% paraformaldehyde overnight, and then sectioned and H&E stained by the UWCCC Experimental Pathology Laboratory. Liver and muscle was embedded in OCT and frozen, and then cryosectioned and Oil-Red-O stained by the UWCCC Experimental Pathology Laboratory. Liver, BAT, and WAT sections were imaged using an EVOS microscope as previously described (Linnemann et al., 2015). Scale bars were inserted automatically or manually by the investigator.

Plasma hormone and lipid measurement

Plasma IGF1 and insulin were quantified according to the manufacturer's protocol using a mouse IGF-1 ELISA kit (80574) and ultrasensitive mouse insulin ELISA kit (90080), respectively, from Crystal Chem. Plasma triglyceride and free fatty acid were assessed according to the manufacturer's protocol using triglyceride colorimetric assay kit (10010303) and free fatty acid fluorometric assay kit (700310) from Cayman Chemical, respectively. Plasma cholesterol was assessed using the stanbio cholesterol liquicolor kit (1010225) from Stanbio Laboratory following to the manufacturer's protocol.

Quantitative PCR

RNA was extracted from liver or adipose tissue using Trireagent according to the manufacturer's protocol (Sigma-Aldrich). The concentration and purity of RNA were determined by absorbance at 260/280 nm using Nanodrop (Thermo Fisher Scientific), and 1 μg of RNA was used to generate cDNA using Superscript III (Invitrogen). Oligo dT primers and primers for real-time PCR were obtained from Integrated DNA Technologies; primer sequences are listed in Table S1. cDNA was diluted 1:15 with water and the diluted cDNA was used for qPCR reactions. Reactions were run on an Applied Biosystems StepOne Plus machine (Applied Biosystems) with Sybr Green PCR Master Mix (Invitrogen) per each manufacturer's instruction (Cummings et al., 2018). β-actin was used to normalize the results from gene-specific reactions.

Immunoblotting

Tissue samples from liver and muscle were lysed in cold RIPA buffer supplemented with phosphatase inhibitor and protease inhibitor cocktail tablets (Thermo Fisher Scientific) as described (Baar et al., 2016) using a FastPrep 24 (M.P. Biomedicals) with bead-beating tubes (16466-042) from (VWR) and zirconium ceramic oxide bulk beads (15340159) from (Thermo Fisher Scientific). Protein lysates were then centrifuged at 13,300 rpm for 10 min and the supernatant was collected. For WAT lysates, protein lysates were then frozen overnight at −80°C, thawed, and the aqueous non-lipids were collected using a needle and syringe; this supplemental step to remove lipids was repeated twice (Baar et al., 2016). Protein concentration was determined by Bradford (Pierce Biotechnology). 20 μg protein was separated by SDS–PAGE (sodium dodecyl sulfate–polyacrylamide gel electrophoresis) on 8%, 10%, or 16% resolving gels (Thermo Fisher Scientific) and transferred to PVDF membrane (EMD Millipore). Membranes were blocked in 5% non-fat dry milk dissolved in TBST for 10 minutes and were then incubated in primary antibody diluted in 5% BSA (for phospho antibodies) or 5% milk (for non-phospho antibodies) overnight. The following commercial primary antibodies were used for immunoblot analysis: RICTOR (1:500; Cell Signaling Technology # 2140), p-S473 AKT (1:1,000; Cell Signaling Technology #4060), p-T308 AKT (1:1,000; Cell Signaling Technology # 2965), AKT (1:1,000; Cell Signaling Technology #4691), HSP90 (1:1,000; Cell Signaling Technology #4877), p-Y1150/1151 IRβ (1:250, Santa Cruz Biotechnology #sc-81500), p-S240/244 S6 ribosomal protein (1:1,000; Cell Signaling Technology #2215), S6 ribosomal protein (1:1,000; Cell Signaling Technology #2217), p-T37/S46 4E-BP1 (1:1,000; Cell Signaling Technology #2855), 4E-BP1 (1:1,000; Cell Signaling Technology #9452), UCP1 (1:500; Abcam #ab10983), and β-actin (1:1,000; Sigma #A2228). Imaging was performed using a GE ImageQuant LAS 4000 imaging station (GE Healthcare). Quantification was performed by densitometry using NIH ImageJ software (Schneider et al., 2012).

Lifespan and necropsy

All mice for the lifespan study were bred by crossing mice homozygous for a conditional allele of *Rictor* (*Rictor*$^{L/L}$) with mice homozygous for a conditional allele of *Rictor* and hemizygous for *Adipoq-Cre* (*Adipoq-Cre; Rictor*$^{L/L}$). Mice were co-housed (grouped by sex and dietary regimen) in SPF housing. Mice were inspected daily and were euthanized for humane reasons if moribund, if the mice developed other specified problems (e.g., excessive tumor burden), or upon the recommendation of the facility veterinarian. Mice found dead were noted at each daily inspection and saved in a refrigerator for necropsy, during which the presence or absence of cancer was recorded. Mice that died during the adaptation to a CR diet, or as a result of the conduct of their cagemates, were excluded from the lifespan analysis. Mice that died within a one week period following the conduct of an *in vivo* procedure, as a result of husbandry errors, or due to anal or uterine prolapse prior to 20 months of age were included and censored as of the date of death. A complete list of mice for the lifespan study is in Table S2.

Frailty

Frailty was assessed longitudinally in a subset of mice using a 26-item frailty index based on the procedures defined by Whitehead et al. (2014). The items scored included alopecia, loss of fur color, dermatitis, loss of whiskers, coat condition, tumors, distended abdomen, kyphosis, tail stiffening, gait disorders, tremor, body condition score, vestibular disturbance, cataracts, corneal opacity, eye discharge/swelling, microphthalmia, vision loss, menace reflex, nasal discharge, malocclusions, rectal prolapse, vaginal/uterine/penile prolapse, diarrhea, breathing rate/depth, and piloerection.

QUANTIFICATION AND STATISTICAL ANALYSIS

Statistical analyses were conducted using Prism 8 (GraphPad Software), except for stratified log-rank survival analyses which were conducted in R (version 3.6.0) using the 'survival' package (version 2.44) (Therneau, 2015). Statistical analyses were performed using two-way ANOVA, with or without repeated-measures as appropriate, and followed by a Holm-Sidak or Tukey-Kramer post-test as specified in the figure legends. Other statistical details can also be found in the figure legends; in all figures, n represents the number of biologically independent animals.

DATA AND CODE AVAILABILITY

This study did not generate/analyze datasets/code.